NEOPLASIA
www.neoplasia.com

Volume 18 Number 10 October 2016 pp. 636–646 636

CXCL1-Mediated Interaction of Cancer Cells with Tumor-Associated Macrophages and Cancer-Associated Fibroblasts Promotes Tumor Progression in Human Bladder Cancer[1,2,3]

Makito Miyake*, Shunta Hori*, Yosuke Morizawa*, Yoshihiro Tatsumi*,†, Yasushi Nakai*, Satoshi Anai*, Kazumasa Torimoto*, Katsuya Aoki*, Nobumichi Tanaka*, Keiji Shimada†, Noboru Konishi†, Michihiro Toritsuka‡, Toshifumi Kishimoto‡, Charles J. Rosser§ and Kiyohide Fujimoto*

*Department of Urology, Nara Medical University, 840 Shijo-cho, Kashihara-shi, Nara 634-8522, Japan; †Department of Pathology, Nara Medical University, 840 Shijo-cho, Kashihara-shi, Nara 634-8522, Japan; ‡Department of Psychiatry, Nara Medical University, 840 Shijo-cho, Kashihara-shi, Nara 634-8522, Japan; §Clinical and Translational Research Program, University of Hawaii Cancer Center, 701 Ilalo St, Rm 327, Honolulu, HI 96813, USA

Abstract

Tumor-associated macrophages (TAMs) and cancer-associated fibroblasts (CAFs) are reported to be associated with poor prognosis, depending on their pro-tumoral roles. Current knowledge of TAMs and CAFs in the tumor microenvironment of urothelial cancer of the bladder (UCB) is limited. Therefore, we investigated the paracrine effect induced by TAMs and CAFs in the tumor microenvironment of human UCB. For this, we first carried out immunohistochemical analysis for CXCL1, CD204 (TAM marker), αSMA (CAF marker), E-cadherin, and MMP2 using 155 UBC tissue samples. Next, CXCL1-overexpressing clones of THP-1-derived TAMs and NIH3T3-derived CAFs were developed by lentiviral vector infection. The immunohistochemical study showed high CXCL1 levels in UCB cells to be associated with enhanced recruitment of TAMs/CAFs, higher metastatic potential, and poor prognosis. Three-dimensional (3D) co-culture of UCB cells and TAMs/CAFs suggested that CXCL1 production in TAMs/CAFs play an important role in cell-to-cell adhesion and interaction among cancer cells and these stromal cells. CXCL1-expressing TAMs/CAFs enhanced tumor growth of subcutaneous UCB tumors in nude mice when injected together. In addition, an experiment using the orthotopic bladder cancer model revealed that CXCL1 production in TAMs/CAFs supported tumor implantation into the murine bladder wall and UCB growth when injected together, which was confirmed by clinical data of patients with bladder cancer. Thus, CXCL1 signaling in the tumor microenvironment is highly responsible for repeated intravesical recurrence, disease progression, and drug resistance through enhanced invasion ability. In conclusion, disrupting CXCL1 signaling to dysregulate this chemokine is a promising therapeutic approach for human UCB.

Neoplasia (2016) 18, 636–646

Introduction

Urothelial cancer of the bladder (UCB) is the second most frequent neoplasm of the urogenital tract, with approximately 74,690 patients and an estimated mortality of 15,580 in 2014 in the US alone [1]. UCB is a heterogeneous disease. Non-invasive, well-differentiated tumors (Ta) are relatively indolent, but T1 high-grade (T1HG)-UCB and muscle invasive bladder cancer (≥T2, MIBC) are known to be life-threatening [2]. Although a multidisciplinary approach has been developed, treatment and management of the disease remains challenging and controversial. To improve the clinical outcome, the

Address all correspondence to Makito Miyake, Department of Urology, Nara Medical University, 840 Shijo-cho, Nara 634-8522, Japan
E-mail: makitomiyake@yahoo.co.jp

[1] Funding: JSPS KAKENHI Grant Number 26861290 (M.M.), 15K10605 (K.F.) and Fiscal Years 2015–2016 Nara Medical University Grant-in-Aid for Collaborative Research Projects (K.F. and M.M.).
[2] Conflicts of interest: The authors disclose no potential conflicts of interest.
[3] Implications: Tumor-associated macrophages and cancer-associated fibroblasts are modulated by a CXCL1 signaling that helps cancer progression, with implications for novel therapeutic opportunities for bladder cancer.
Received 29 April 2016; Revised 5 August 2016; Accepted 11 August 2016

1476-5586
http://dx.doi.org/10.1016/j.neo.2016.08.002

mechanisms underlying tumor invasion, metastasis, and treatment resistance need to be elucidated.

Tumor tissue is composed of cancer cells and various types of stromal cells, including endothelial cells, macrophages, and fibroblasts. Their interaction and crosstalk might lead to the formation of a cancer-specific microenvironment for tumor progression. Tumor-promoting inflammation is known to be one of the hallmarks of malignancy [3]. Complexity arises from various types of inflammatory cells, chemokines, and cytokines in solid tumors and their surrounding areas [4]. The intravesical instillation of Bacillus Calmette–Guérin (BCG) has been used as an effective immunotherapy to prevent tumor recurrence and progression in selected patients with non-muscle invasive bladder cancer (NMIBC) [2], implying that UCB is a potentially immunogenic disease. Recently, we reported that the expression of chemokine (C-X-C motif) ligand 1 (CXCL1) is associated with tumor aggressiveness and angiogenesis in human UCB and prostate cancer [5–7]. However, only limited data are available on the biological role and paracrine network of CXCL1 in the tumor microenvironment of human UCB.

Macrophages are the most abundant stromal cells associated with the host immune system in the tumoral area, and they have diverse phenotypes. In the oncology field, macrophages have 2 different functions, a tumor-suppressive (M1) and a tumor-supportive (M2) function, which could be a consequence of the different tumor microenvironments [8,9]. Tumor-associated macrophages (TAMs, also known as M2 macrophages) are recognized to be oriented towards promoting tumor growth through enhanced tumorigenesis, angiogenesis, and suppression of adaptive immunity (M2 function). TAMs recruited by chemokines such as interleukin (IL)-4 and IL-13 are a major component of the leukocyte infiltrate in tumors [9,10]. A high density of tumor-infiltrating TAMs has been shown to be associated with poor outcomes in various types of cancer, including UCB [11–14]. Fibroblasts are among the most active cell types of the stroma and perform tissue repair functions under certain physiological conditions [15]. Cancer-associated fibroblasts (CAFs, also known as myofibroblasts) are another major component in the tumor stroma and play a critical role in tumor growth, angiogenesis, and treatment resistance by secreting cytokines such as CXCL12, favoring a variety of tumor-specific mechanisms like epithelial–mesenchymal transition (EMT) [16,17]. Their roles consist of creating a structural matrix around cancer cells, recruiting new blood vessels, and stimulating the production of proteases that can degrade adjacent tissues, thereby increasing the likelihood of tumor development, invasion, and metastasis [18]. A number of studies addressing the prognostic impact of CAFs in human malignancies, including UBC, have shown an association between a high density of CAFs and poor prognosis [19–21]

A complete understanding of the molecular mechanism driving the interaction and crosstalk between tumor cells and TAMs/CAFs is essential for overcoming treatment resistance and improving patient outcome. To date, no study has focused on how TAMs and CAFs modulate the aggressiveness of UCB in the mediation of CXCL1. In the present study, we investigated the role of the paracrine effect induced by TAMs and CAFs in the tumor microenvironment of human UCB.

Materials and Methods

Patient Selection and Data Collection

The Ethics Committee of the Nara Medical University approved this study, and all participants provided informed consent. The study was conducted on 155 patients with pathologically diagnosed primary NMIBC who underwent transurethral resection of bladder tumor (TURBT) between January 2004 and April 2013. The clinical information and follow-up data were collected by retrospective chart review. All hematoxylin and eosin (H&E)-stained specimens obtained by initial TURBT were reassessed independently by 2 experienced uropathologists (K.S. and N.K.) with regard to T category (2010 American Joint Committee on Cancer TNM Staging system), tumor grade (2004 WHO classification), and lymphovascular invasion. Follow-up was performed according to our institutional protocol [2]. Progression was defined as recurrent disease when there was invasion into the muscularis propria (≥T2), positive lymph nodes, and/or the occurrence of distant metastases.

Immunohistochemical Staining and Quantification

Immunohistochemical (IHC) staining using paraffin-embedded, formalin-fixed tissue blocks was performed as previously described [5]. Antibodies and treatment details are available in the Supplementary Table S1. CXCL1 expression in cancer cells was semi-quantified as previously described [5]. The proportion and intensity scores were added to obtain a combined score as follows: low, intermediate, and high. CD204-positive round cells in the cancerous area were counted in at least 3 independent high-power microscopic fields (HPF; 400×, 0.0625 μm^2) [14]. The mean number of macrophages was calculated as tumor-infiltrating TAMs. The immunoreactivity of αSMA at the tumor border was scored according to the number of αSMA-positive spindle cells (CAFs) as follows: 0, almost no CAFs or a small number of CAFs surrounding less than half of the border; 1, a moderate number of CAFs surrounding less than half of the border; or 2, a large number of CAFs surrounding more than half of the border [22]. To quantify the expression level of MMP2, E-cadherin, and IL-6 in UBC cells, immunoreactive tumor cells were counted in at least 3 independent fields, and the percentage of positive cells was calculated by dividing that number by the total counted cancer cells (1–100%). Evaluation was carried out by 2 investigators (M.M. and Y.T.) blindly, without knowledge of the patients' outcome or other clinicopathological characteristics.

Cell Lines and Reagents

Four bladder cancer cell lines, J82, UMUC3, T24 (ATCC, Manassas, VA, USA), MGH-U3 (a generous gift from Dr H. LaRue at Laval University Cancer Research Centre, Quebec, Canada), benign bladder cell line UROtsa (a generous gift from Dr Donald Sens at the University of North Dakota School of Medicine, Grand Forks, ND, USA), acute monocytic leukemia cell line THP-1 (ATCC), mouse dermal fibroblast cell line NIH3T3 (ATCC), and HEK293FT (Invitrogen, Carlsbad, CA, USA) were used in the present study. Cell lines were authenticated by analysis of their genetic alterations. Cell lines were maintained in DMEM or RPMI-1640 media supplemented with 10% fetal bovine serum (FBS), 100 units/mL penicillin, and 100 μg/mL streptomycin in a standard humidified incubator at 37°C in 5% CO_2.

Phorbol-12-myristate-13-acetate (PMA) was purchased from Cell Signaling Technology (Beverly, MA, USA). Recombinant proteins, CXCL1 (R&D Biosystems, Minneapolis, MN, USA), TGF-β (Wako Pure Chemical, Osaka, Japan), IL-4, and IL-6 (Prospec, East Brunswick, NJ, USA) were used in the described experiments.

Western Blot Analysis

Western blotting was performed as previously described [23]. The primary antibodies used in this study were anti-CXCL1 (dilution, 1:500), anti-CD204 (dilution, 1:2,000), anti-αSMA (dilution, 1:10,000), and anti-actin antibody (dilution, 1:20,000; clone AC-15, Sigma-Aldrich, St Louis, MO, USA) as an internal loading control.

Generation of TAMs from THP-1 and CAFs from NIH3T3

To generate TAMs from monocytic THP-1, cells were seeded at 2×10^5 cells/cm^2 and treated with PMA (200 nM) for 24 h for differentiation into resting macrophages (M0 cells). For M2 polarization, cells were treated with IL-4 (20 ng/mL) for an additional 48 h. To generate CAFs from NIH3T3, 70% confluent cells grown on dishes or flasks were activated with TGF-β (20 ng/mL) for 48 h. To confirm the generation of TAMs and CAFs, western blot analysis for CD204 and αSMA, respectively, was performed.

Dual Immunofluorescence Staining of Human Bladder Cancer Tissue

Dual immunofluorescence staining was performed with antibodies specific to CXCL1/CD204 or CXCL1/αSMA (goat polyclonal/mouse monoclonal). Briefly, paraffin sections were placed on glass slides and subjected to deparaffinization and antigen retrieval with citric acid, followed by blocking in 1% BSA for 1 h. The sections were incubated in anti-CXCL1 (dilution, 1:100) and CD204 (dilution, 1:200) or αSMA (dilution, 1:1,000) for 1 h at room temperature and rinsed thrice in PBS. The sections were incubated in Alexa Fluor 594 anti-goat IgG and Alexa Fluor 488 anti-mouse IgG secondary antibody (dilution, 1:500; Life Technologies) for 30 min and mounted with mounting medium with DAPI (Vector Laboratories, Burlingame, CA, USA). The sections were immediately examined under a fluorescence microscope (Leica DMI 4000B, Wetzlar, Germany).

Real-Time Reverse Transcription PCR

RNA extraction and real-time RT-PCR were performed as previously described [23].

The gene-specific TaqMan primer and probe sets used in this study were Hs00236937_m1 for human CXCL1, Hs01891184_s1 for human CXCR2, Hs01060665_g1 for human β-actin, Mm04207460_m1 for mouse CXCL1, Mm99999117_s1 for mouse CXCR2, and Mm01324804_m1 for mouse β-actin. Relative fold changes in mRNA levels were calculated after normalization to β-actin using the comparative Ct method.

Lentivirus Production and Infection for CXCL1 Overexpression

For lentivirus production, CXCL1 expression vector (EX-G0095-Lv105) or its empty control (Lv105CT; GeneCopoeia, Rockville, MD, USA) and Virapower packaging mix plasmids (pLP1, pLP2, and pLP/VSVG; Life Technologies) were mixed and transfected into 293FT cells using Calphos Mammalian Transfection Kit (Clontech, Palo Alto, CA, USA) according to the manufacturer's instructions. Forty-eight hours after transfection, the supernatant containing the lentivirus was produced in HEK-293FT, collected, and filtered. The culture medium of THP-1 and NIH3T3 cells seeded on 35-mm dishes was half-replaced with virus-containing supernatant supplemented with 4 μg/mL polybrene and incubated overnight. Then, medium was replaced, and stable transfectants were selected with 2 μg/mL of puromycin (Sigma-Aldrich) for 14 days and subcloned by limiting dilution in 96-well plates. Integration of the transfected gene was confirmed by western blotting. Stable cell lines were maintained in media containing 2 μg/mL of puromycin for THP-1 and NIH3T3 clones.

Cell Invasion Assay Using Conditioned Media Obtained from TAMs and CAFs

THP-1-derived TAMs or NIH3T3-derived CAFs were seeded onto 6-well plates at a density of 200,000 cells/well in serum-containing media. Twenty-four hours later, the medium was replaced with serum-free RPMI1640 medium, and cells were incubated for additional 48 h. The conditioned medium was collected from manipulated TAMs and CAFs, followed by centrifugation to remove cells or cell debris. The invasion assay was performed with the BD Falcon FluoroBlok Insert System according to the manufacturer's directions. Briefly, 24-well plates with 8-μm pore membranes were coated with 200 ng/mL growth factor reduced Matrigel (BD Biosciences, San Jose, CA). MGH-U3 or T24 cells were added to each insert at a density of 25,000 cells/well in the conditioned media described above. The lower chamber contained RPMI1640 media with 10% FBS as a chemoattractant. The cells were maintained in a humidified incubator with 5% CO_2 at 37°C for 48 h. The cells attached to the bottom of the membrane were stained for 30 min with the cell viability indicator Calcein AM Fluorscent Dye (PromoKine, Heidelberg, Germany) and quantified using a microplate spectrophotometer (Infinite 200M PRO; Tecan, Männedorf, Switzerland) at 495 mm excitation and 515 nm emission. Cells were examined by fluorescent microscopy.

Three-Dimensional Co-Culture of Urothelial Cancer Cells and TAMs/CAFs

UCB cells (MGH-U3 and T24) and THP-1-derived TAMs or NIH3T3-drived CAFs were co-cultured on 96-well NanoCulture plate with a micro-square pattern (SCIVAX, Kanagawa, Japan). Before seeding, UCB cells were labeled with the green-fluorescent dye PKH-67 (Sigma-Aldrich), and TAMs/CAFs were labeled with the red-fluorescent dye PKH-26 (Sigma-Aldrich). UCB cells and TAMs or CAFs (CXCL1 expression or empty control) seeded at the same cell number (5×10^3 cells/well) were plated and incubated for 3 days. Anti-CXCL1-neutralizing antibody (ab89318; Abcam, Cambridge, MA, USA) was used to inhibit CXCL1 function in the co-culture experiments. Spheroid formation was examined by fluorescent microscopy.

Animal Experiments and Monitoring

Approval for the animal studies was obtained from the Committee on Animal Research of the Nara Medical University. Specific pathogen–free 6-week-old athymic BALB/c nu/nu mice and C.B-17/severe combined immunodeficiency (SCID) mice were used (Oriental Bio Service, Kyoto, Japan). At least 8 animals were included in each group.

The subcutaneous tumorigenicity assay was performed in nude mice by injecting bladder cancer cells (1×10^6) and TAMs or CAFs (0.5×10^6) in a 1:1 mixture of Matrigel. Tumor diameters were measured twice a week with electronic calipers, and tumor volumes were calculated using the following formula: $\{(\text{width})^2\times\text{length}\}/2$ (mm^3). The mice were killed on day 21, and the tumors were resected for IHC staining analysis. To generate the orthotopic bladder tumor models, UMUC3 (2×10^6) and TAMs or CAFs (1×10^6) were injected into the bladder cavity of SCID mice by 24-gauge angiocatheters (Surflo; Terumo Corp, Tokyo, Japan) as described previously [24]. Two weeks

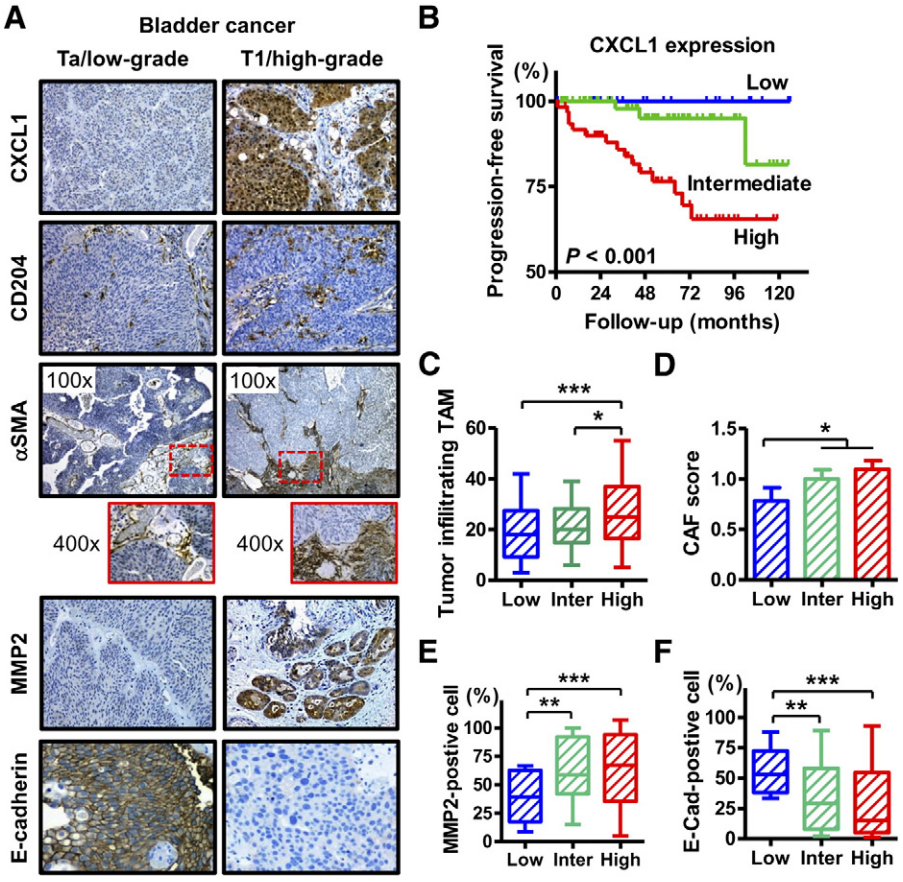

Figure 1. CXCL1 expression and recruitment of stromal cells in human non-muscle invasive bladder cancer. (A) Representative expression status of CXCL1, CD204, αSMA, MMP2, and E-cadherin in human bladder cancer tissues. All images were captured at 200× magnification except for αSMA, for which the images were captured at 100× and 400× magnification. (B) Progression-free survival curves of patients with NMIBC after TURBT according to the expression level of CXCL1. (C–F) comparison of CXCL1 expression levels with (C) the number of tumor-infiltrating TAMs, (D) induction level of CAFs (CAF score), (E) percentage of MMP2-positive cells, and (F) percentage of membranous E-cadherin-positive cells. In the box-and-whisker plot or bar charts, significance (* $P < 0.05$, ** $P < 0.05$) was assessed by the Mann–Whitney *U* test.

after cell injection, the bladders of the mice were resected to evaluate the intravesical tumor implantation rate by H&E staining and assessed by IHC for CD204, αSMA and E-cadherin.

Statistical Analysis

Progression-free survival (PFS) and intravesical recurrence-free survival from the day of initial TURBT were obtained using the Kaplan–Meier method and compared by the log-rank test or log-rank test for trend. Data are expressed by bar charts or box plots, and Student's *t*-test or the Mann–Whitney *U*-test was applied for statistical analysis as appropriate. The interrelationship between IL-6 expression and tumor-infiltrating TAM was examined using Spearman's correlation. IBM SPSS Version 21 (SPSS Inc., Chicago, IL, USA) and PRISM software version 5.00 (San Diego, CA, USA) were used for statistical analyses and plotting the data, respectively. $P < 0.05$ was considered statistically significant.

Results

Correlation of CXCL1 Expression with Clinicopathological Features and Treatment Outcome in NMIBC

The clinicopathological characteristics of 155 NMIBC cases are outlined in Supplementary Table S2. Representative images of IHC staining of CXCL1, CD204, αSMA, MMP2, and E-cadherin are shown in Figure 1A. CXCL1 was expressed predominantly in the cytoplasm of tumor cells. Strong CXCL1 expression was observed in the tumor tissue of the T1 high-grade tumors, whereas the expression level of CXCL1 was relatively lower in the Ta low-grade tumors (Figure 1A, first panel). When compared with clinicopathological variables, a higher CXCL1 expression score was associated with higher T category and tumor grade (Supplementary Table S2. In addition, Kaplan–Meier analysis showed that a high CXCL1 expression score was associated with a high risk of disease progression (Figure 1B).

Next, quantitative assessment of TAM, CAF, MMP2, and E-cadherin expression was performed and compared with the CXCL1 expression score. Higher levels of CXCL1 expression in the tumors were associated with a higher number of tumor-infiltrating TAMs (Figure 1C), enhanced recruitment of CAFs to the tumoral area (Figure 1D), higher expression of MMP2 (Figure 1E), and lower expression of E-cadherin (Figure 1F). These findings suggest that CXCL1 expression in cancer cells exhibits aggressiveness and poor clinical outcome by modifying the tumor microenvironment.

Induction of TAMs and CAFs by IL-6 Overexpression

Conversion into TAMs and CAFs has been found to be involved in IL-6 expression in some types of malignancy [9,25]. To investigate whether IL-6 expression in human UCB was associated with the conversion, additional IHC analysis was performed. Figure 2A shows

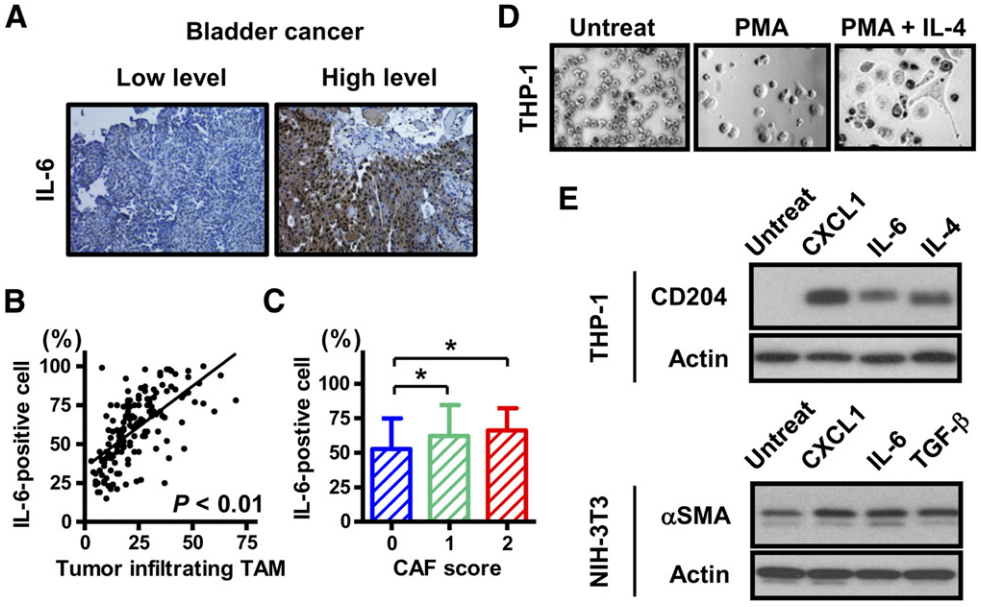

Figure 2. Induction of TAMs and CAFs by IL-6 in human bladder cancer tissues and confirmation by *in vitro* experiments. (A) Representative expression status for IL-6 in human bladder cancer tissues. Images were captured at 200× magnification. (B) The interrelationship between the percentage of IL-6-positive cancer cells and the number of tumor-infiltrating TAMs was examined using Spearman's correlation. Spearman r was found to be 0.68 (95% confidence interval, 058–0.76). (C) Comparison of the percentage of IL-6-positive cancer with the induction level of CAFs (CAF score). (D) Morphological changes of THP-1 cells by PMA and IL-4 treatment. THP-1 cells were treated with 200 nM PMA for 24 h to differentiate them into resting macrophages (middle), followed by treatment with IL-4 (20 ng/mL) for 48 h (right). (E) Western blot analysis for confirming the generation of TAMs and CAFs. THP-1 cells were treated with a combination of PMA and 20 ng/mL of CXCL1, IL-6, or TGF-β, separately. Upregulation of CD204 indicates differentiation into TAMs. NIH3T3 cells were treated with 20 ng/mL of CXCL1, IL-6, or TGF-β, separately. Upregulation of αSMA indicates the activation of fibroblasts, which are known to be CAFs.

representative images for low and high expression of IL-6. A higher rate of IL-6-positive cells was correlated with higher tumor-infiltrating TAM or higher CAF score (Figure 2B and C). To confirm the generation of TAMs from THP-1, THP-1 cells were treated with PMA alone or PMA+IL-4. PMA treatment induced resting macrophages (M0 cells), and PMA treatment followed by IL-4 stimulation induced growing M2 macrophages (Figure 2D). Before treatment, THP-1 cells were round, floating, and did not attach to the bottom surface of the culture dish. After treatment with TPA and IL-4, they adhered to the bottom surface with abundant cytoplasmic projections. Western blot analysis revealed that, like IL-4, CXCL1 or IL-6 stimulation upregulated the CD204 expression of THP-1, suggesting that both CXCL1 and IL-6 were potential inducers of TAM from monocytes (Figure 2E). Morphological changes similar to those observed with IL-4 treatment were found with CXCL1 and IL-6 treatment as well. In addition, like IL-4, CXCL1 or IL-6 stimulation upregulated αSMA expression in NIH3T3 cells, suggesting that both CXCL1 and IL-6 were potential inducers of CAFs from normal fibroblasts (Fig. E). These results implied that both CXCL1 and IL-6 from cancer cells were associated with recruitment and induction of TAMs and CAFs in human UCB.

CXCL1 Produced by TAMs and CAFs Around the Tumoral Area Promotes the Invasion Capability of UCB

To investigate whether TAMs and CAFs around the tumoral area produce CXCL1, dual immunofluorescence staining was performed with antibodies specific to CXCL1/CD204 or CXCL1/αSMA. The representative images from fluorescent microscopy showed that some TAMs and CAFs around the tumoral area produced CXCL1.

To explore the role of CXCL1-expressing TAMs and CAFs in the tumor microenvironment of UBC, cell line-based experiments were performed. The endogenous expression levels of CXCL1 and CXCR2 in 5 epithelial cell lines, as well as the THP-1 and NIH3T3 cell lines, were evaluated by real-time RT-PCR. J82, UMUC3, and T24 (known as poorly differentiated high-grade UCs) expressed higher levels of CXCL1 compared to UROtsa (derived from normal urothelia) and MGH-U3 (derived from low-grade/low-stage UC). There was no endogenous expression of CXCL1 in THP-1 or NIH3T3 cells (Figure 3B). CXCR2 was expressed in all the cell lines, whereas a slightly higher expression level of CXCR2 was observed in MGHU3, THP-1, and NIH3T3 cells compared to that in UROtsa, J82, UMUC3, and T24 cells (Supplementary Figure S1).

After lentiviral infection and puromycin selection, CXCL1 expression and CD204/αSMA markers were confirmed by western blotting analysis. CXCL1 expression occurred in LvCXCL1-THP-1 and LvCXCL1-NIH3T3 as opposed to no expression in the corresponding controls (LvNega). The induction of CXCL1 in NIH3T3 cells resulted in slightly elevated αSMA (Figure 3C). Following our hypothesis that high CXCL1 production in the TAMs and CAFs around the tumoral area would enhance tumor invasiveness, an *in vitro* invasion assay was carried out. In the invasion assay, we treated MGH-U3 and T24 bladder cancer cells with conditioned media obtained from manipulated THP-1-derived TAMs and NIH3T3-derived CAFs infected with the lentiviral vector. The invasion capability of both UCB cells was significantly enhanced when treated with media from LvCXCL1-TAMs and LvCXCL1-CAFs (Figure 3D).

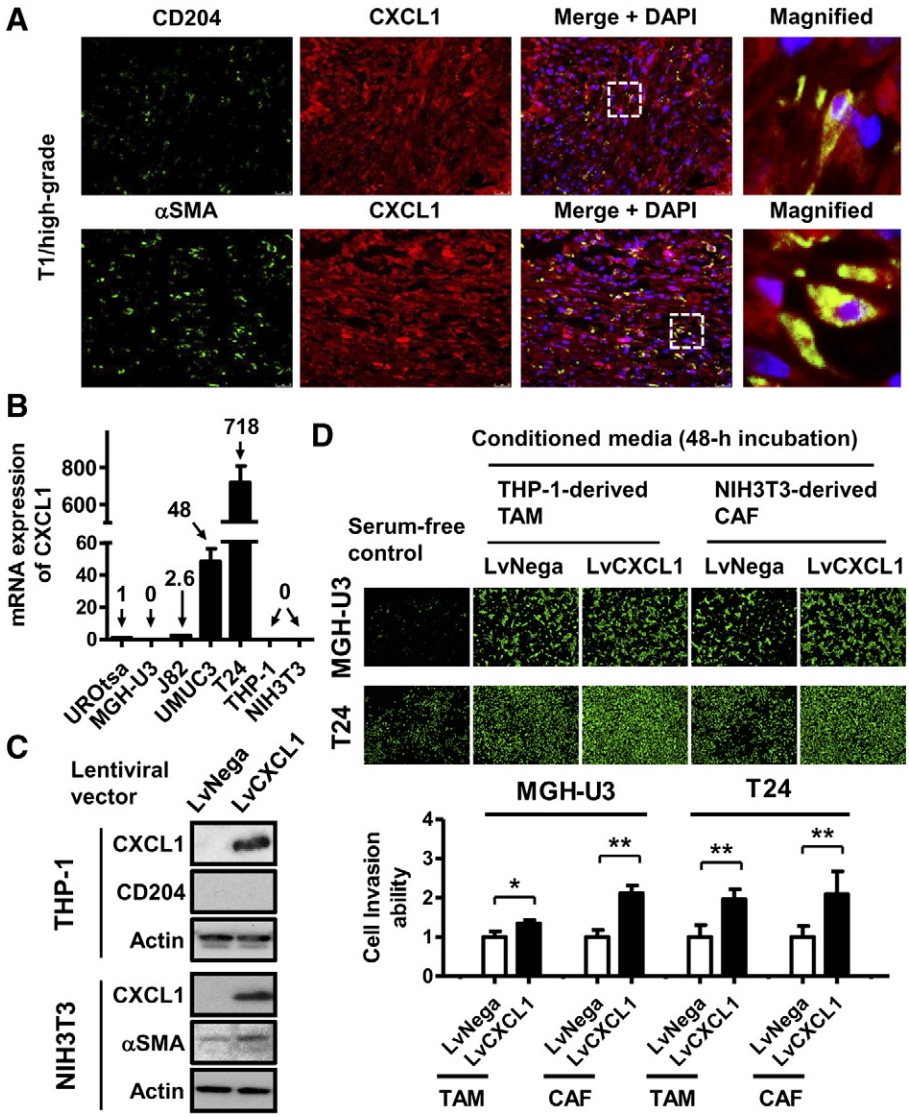

Figure 3. Association of CXCL1 production in TAMs/CAFs with invasion potential of human bladder cancer. (A) Dual immunofluorescence staining analysis for CD204 or αSMA (green) and CXCL1 (red) shows the expression of CXCL1 in TAMs and CAFs in the tumoral area. Overlay images and their magnified images are shown (2 panels on the right). Original magnification, 200×. (B) CXCL1 mRNA expression level was determined by real-time RT-PCR. Expression levels are the result of 3 experiments and are expressed as the mean ± SD relative to that of UROtsa, which is defined as 1. (C) THP-1 and NIH3T3 cells were infected with lentiviral constructs harboring empty vectors (LvNega) or CXCL1 expression vectors (LvCXCL1). Western blot analysis demonstrated altered CXCL1 expression in both cell lines. The changes in the expression levels of CD204 and αSMA were evaluated in infected THP-1 and NIH3T3 cells, respectively. Actin served as the loading control. (D) MGH-U3 and T24 cells were suspended in the conditioned media collected from manipulated TAMs and CAFs and subjected to *in vitro* invasion assays. Data are expressed as the mean ± SD of 3 independent experiments conducted in triplicate; *, $P < 0.05$, **, and $P < 0.01$.

CXCL1 Production in TAMs and CAFs Correlates with the Adhesion of Bladder Cancer Cells with TAMs and CAFs

To recognize the cell-to-cell adhesion between UCB cells and TAMs or CAFs in 3D co-culture, CXCL1-expressing TAMs and CAFs were mixed with UCB cells and seeded. These cells were identified by a dual fluorescence detection method. Representative pictures of co-localization and adhesion of UCB cells/TAMs and UCB cells/CAFs are shown in Figure 4. As compared with empty vector-transfected TAM (LvNega-TAM), the cell-to-cell adhesion rate of UCB cells/TAMs was significantly greater and formed more homogenous and larger spheroids in LvCXCL1-TAM (Figure 4A). Despite the endogenous expression of CXCL1 in T24 cells (Figure 3B), CXCL1 produced by TAMs has a significant role in the adhesion between UCB cells and TAMs. Notably, adhesion between UCB cells and TAMs and the growth of spheroids were significantly inhibited by treatment with anti-CXCL1-neutralizing antibody (Figure 4B). UCB cells and TAMs did not merge but, instead, separately formed spheroids of each cell type. Similar results were obtained in the experiments for adhesion and interaction between UCB cells and CAFs (Figure 4C and D). These findings suggested that both of CXCL1 produced by UCB cells and CXCL1 produced by TAMs or CAFs play an important role in the adhesion and interaction between these cells.

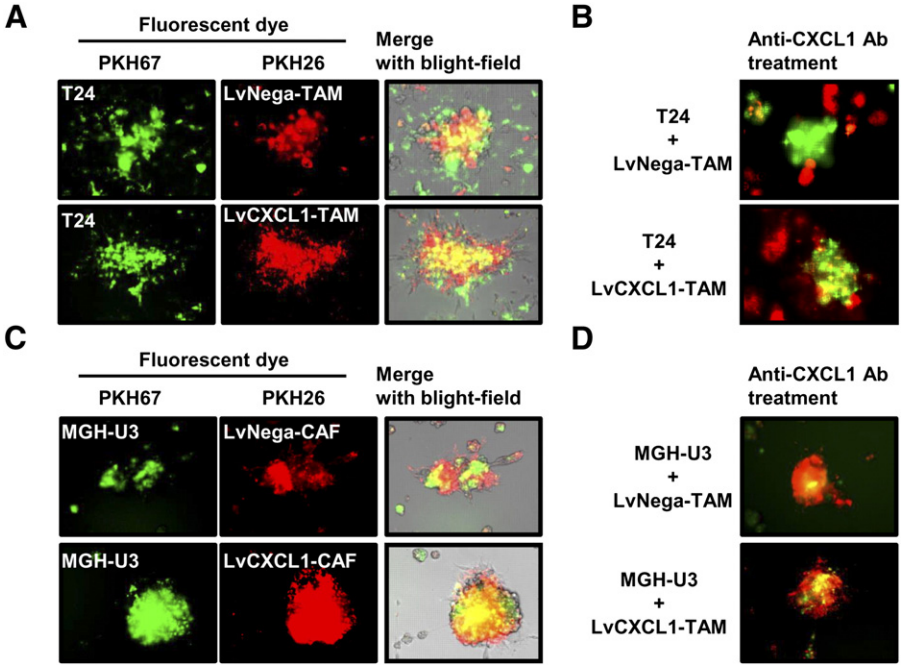

Figure 4. Association of CXCL1 production in TAMs/CAFs with strong adhesion to bladder cancer cells and formation of homogenous multicellular spheroids. Bladder cancer cells T24 and MGH-U3 were labeled with PKH67 (green dye). THP-1-derived TAMs and NIH3T3-drived CAFs were labeled with PKH26 (red dye). After labeling, cancer cells and stromal cells were mixed at the same number (5×10^3 cells/well) and plated into a 3D culture plate. Photographs of randomly selected spheroids were captured 3 days after plating. Representative spheroids are shown as follows: (A) spheroids of the co-culture of T24 cells and TAMs; (B), spheroids of T24 cells and TAMs treated with anti-CXCL1-neutralizing antibody; C, spheroids of the co-culture of MGH-U3 cells and CAFs; (D) spheroids of MGH-U3 cells and CAFs treated with anti-CXCL1-neutralizing antibody. Original magnification, 400×.

CXCL1 Production in TAMs and CAFs Enhances Tumor Growth and Intravesical Implantation in in Vivo Bladder Cancer Models

To investigate the *in vivo* influence of CXCL1 production in TAMs and CAFs, we used 2 different types of *in vivo* experimental models of bladder cancer. In the subcutaneous xenograft model, we inoculated bladder cancer cells together with the manipulated TAMs or CAFs. The proliferation ability of the mixture of LvCXCL1-TAMs/LvCXCL1-CAFs and cancer cells was significantly higher than that of the mixture of LvNega-TAMs/LvNega-CAFs and cancer cells or cancer cells only (Figure 5A-D). The difference in 21-day tumor size between LvCXCL1-TAMs and LvNega-TAMs, as well between LvCXCL1-CAFs and LvNega-CAFs, was more pronounced in MGH-U3 than in UMUC3. IHC staining for CD204, αSMA, and E-cadherin demonstrated that CXCL1 overexpression in TAMs and CAFs enhanced subcutaneous tumor growth of bladder cancer cell lines by increased recruitment of stromal cells, EMT promotion by decreased membranous expression of E-cadherin, and increased invasion phenotype by MMP2 expression. There were higher numbers of tumor-associated stromal cells in the tumors inoculated with CXCL1-overexpressing TAMs and CAFs (Figure 5E).

Next, we used the orthotopic bladder cancer model with SCID mice to evaluate the potential of implantation in the bladder. We inoculated UMUC3 bladder cancer cells into the murine bladder together with the manipulated TAMs or CAFs. Two weeks after inoculation, the bladders were resected, and tumor implantation was identified by H&E staining. We pathologically confirmed the successful implantation of UMUC3 cells in murine bladders (Figure 5F). Bladder tumors inoculated with LvCXCL1-TAMs and LvCXCL1-CAFs were apparently larger than those inoculated with control cells (LvNega). The implantation rate was significantly higher in the murine bladders inoculated with TAM- and CAF-LvCXCL1 as compared to those inoculated with control cells (Figure 5G). In the intravesical inoculation of the mixture of cancer cells and TAMs, 3 out of 8 murine bladders (37.5%) harbored tumors, whereas 6 out of 8 (75.0%) did not. Regarding the CAFs, 2 out of 8 murine bladders (25.0%) harbored tumors, whereas 7 out of 8 (87.5%) did not. Thus, CXCL1 production in the TAMs and CAFs supports the attachment of bladder cancer cells to the bladder wall and the consequent tumor growth in the orthotopic bladder condition. To investigate whether higher levels of tumor-infiltrating TAMs and CAFs around the tumoral area are associated with a higher risk of bladder cancer recurrence after TURBT in human NMIBC, recurrence-free survival curves were generated and compared by the number of TAMs and the CAF score in the IHC staining (Figure 5H). Higher number of TAMs (≥25 TAMs/HPF) correlated with a higher risk of bladder cancer recurrence ($P = 0.03$), while an increased risk of bladder cancer recurrence in the tumors with high levels of CAF (CAF score = 2) was observed as compared to those with low levels of CAF (CAF score = 0/1); however, the difference did not reach statistical significance ($P = 0.18$).

Discussion

CAFs have been reported to contribute to a tumor-permissive inflammatory environment, while TAMs display immunosuppressive and tumor-promoting behaviors, including pro-metastatic function by the expression of angiogenesis factors and MMPs [20]. Although many efforts have been made to clarify the crosstalk and interaction between these stromal cells and cancer cells, the complete picture remains obscure. Considering that intravesical instillation of BCG is widely used as an effective immunotherapy, bladder cancer cells have a strong linkage to inflammatory and immunologic cells. Moreover, several recent clinical trials for novel immunotherapies targeting

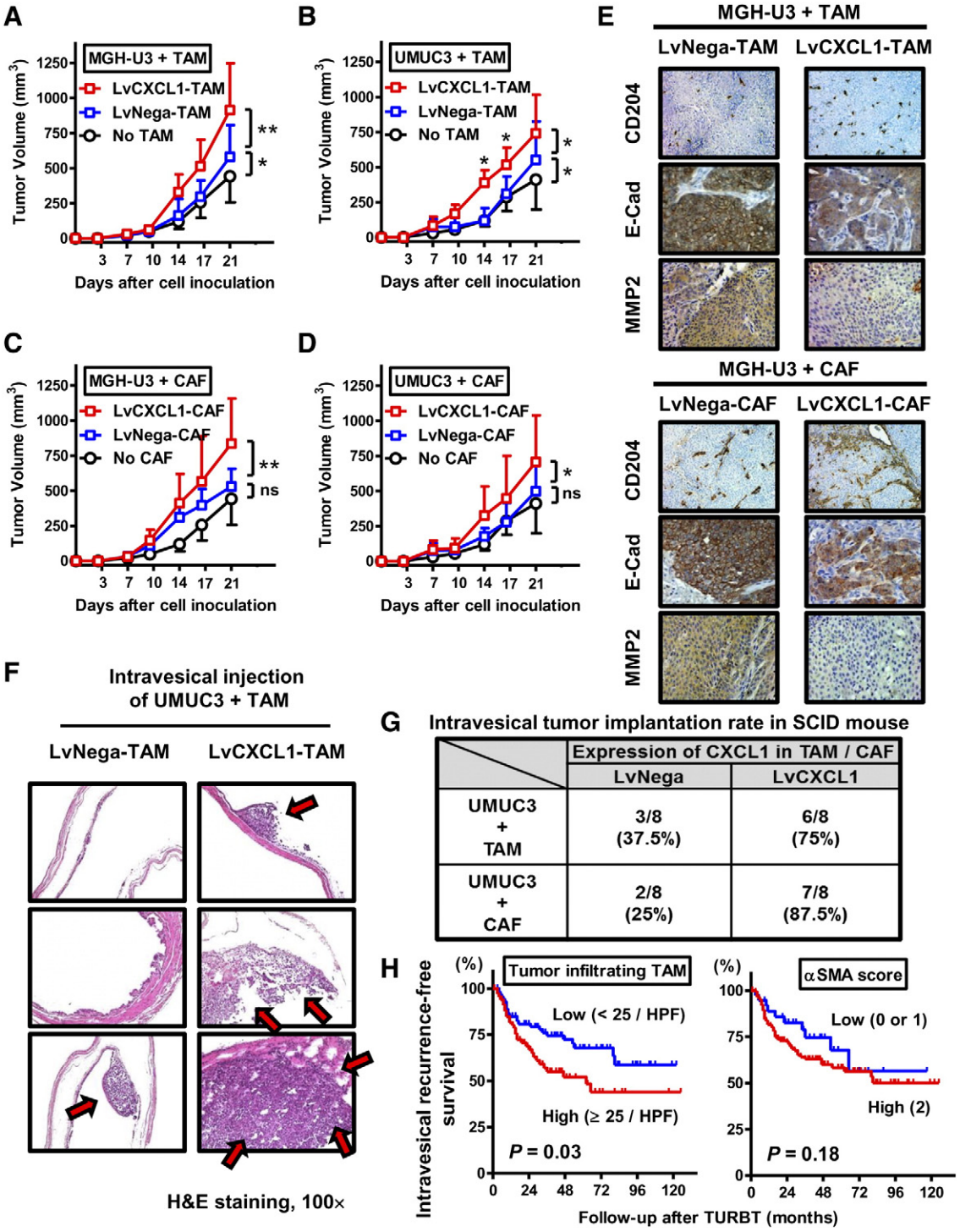

Figure 5. Subcutaneous xenograft models and orthotopic bladder cancer models using human bladder cancer cells, TAMs, and CAFs. (A) MGH-U3 cells (1×10^6) mixed with LvCXCL1-TAMs or LvCXCL1-TAMs (0.5×10^6) and MGH-U3 cells (1×10^6) not mixed with TAM were injected subcutaneously into athymic nude mice. Similar experiments were conducted using UMUC3 cells and TAMs (B), MGH-U3 cells and CAFs (C), and UMUC3 cells and CAFs (D). Tumor size, recorded over 21 days, was plotted as mean ± SD for the 3 groups (n = 8/group). Tumor sizes on the 21st day were compared by the Mann–Whitney *U* test (* $P < 0.05$, ** $P < 0.05$; ns = no significance). (E) The resected tumors were analyzed by immunohistochemical staining for CD204, αSMA, E-cadherin, and MMP2. Representative pictures for tumors of MGH-U3/TAMs and MGHU-3/CAFs are shown. (F and G) The orthotopic models using SCID mice were generated by injecting the mixture of MGH-U3 cells (2×10^6) and the manipulated TAMs or CAFs (1×10^6). Two weeks after injection, the bladders of mice were resected to evaluate intravesical tumor implantation rate by H&E staining for each group (n = 8/group). (H) Intravesical recurrence-free survival curves in patients with NMIBC after TURBT according to the number of tumor-infiltrating TAMs (left) and the CAF score (right).

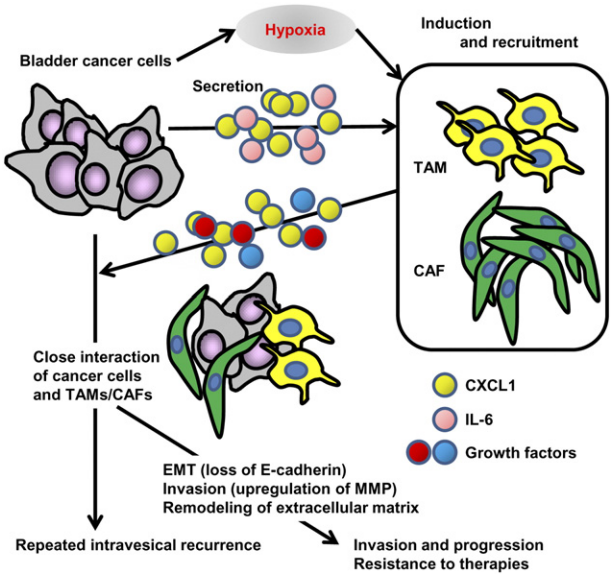

Figure 6. Schematic diagram of the proposed mechanism for crucial roles of CXCL1 in human urothelial carcinoma of the bladder. TAM, tumor-associated macrophage; CAF, cancer-associated fibroblast; CXCL1, chemokine (C-X-C motif) ligand 1; MMP, matrix metalloprotease.

CTLA-4 and PD1/PD-L1 have shown promising clinical outcomes [26–28]. However, some of the treated patients experience disease relapse or treatment failure. The molecular mechanisms of how stromal cells like CAFs and TAMs in UCB affect aggressiveness and resistance to these immunotherapies needed to be unveiled to improve the clinical outcome.

In an earlier study, we found that the expression of CXCL1 was associated with tumor aggressiveness and angiogenesis in human UCB [5,7]. In 2012, Acharyya *et al.* demonstrated that elevated CXCL1 attracts CD11b+Gr1+ myeloid cells into the tumor, which produce chemokines, including S100A8/9, resulting in breast cancer cell survival [29]. The authors concluded that this network of endothelial-carcinoma-myeloid signaling interactions was associated with chemoresistance and metastasis through the CXCL1/2-S100A8/9 loop. However, there is only limited information about the role of CXCL1 on the paracrine network in the tumor microenvironment of human UCB. Thus, we first investigated whether the CXCL1 expression level in UCB influenced TAM and CAF recruitment and metastatic potential using E-cadherin and MMP2, which are known as prognostic markers of UCB. Robust associations of higher CXCL1 expression with enhanced recruitment of both TAMs and CAFs, higher metastatic potential, and decreased PFS were observed (Figure 1). MMP2 has been suggested to play essential roles in tumor invasion and progression. TAMs and CAFs around the tumors produce growth factors, chemokines, and extracellular matrix components such as collagen I/IV, fibronectin, and tenascin-C. They also secrete protein acidic and rich in cysteine (SPARC), which might be facilitating the angiogenic recruitment of endothelial cells and pericytes [30]. This dynamic reprogramming is regulated by membrane type 1 matrix metalloproteinase (MT1-MMP), which triggers tumor invasion indirectly by activating MMP2 function and directly by degrading the extracellular matrix [31]. Moreover, pre-metastatic niches formed by invading bone marrow-derived cells (BMDCs) facilitate tumor cells to metastasize. Lysyl oxidase plays a critical role for pre-metastatic niche formation. High levels of MMP2 leads to the cleavage of collagen IV, thereby enhancing the invasion and recruitment of additional BMDCs and metastasizing tumor cells [32].

In previous studies, polarization/activation of TAMs and induction/recruitment of CAFs were found to be regulated by tumor cell-derived molecules such as IL-6 [11,33]. We hypothesized that IL-6 signaling from bladder cancer cells mediates the recruitment of these stromal cells. IHC staining analysis showed a positive relationship between IL-6 expression levels of cancer cells and induction levels of TAMs/CAFs (Figure 2A–C). In addition, IL-6 stimulation, as well as CXCL1 stimulation, upregulated CD204 and αSMA expression levels in THP-1-derived macrophages and NIH3T3-derived CAFs, respectively. These findings suggest that besides CXCL1 paracrine signaling, IL-6 signaling between cancer cells and stromal TAMs/CAFs could represent a key factor for creating the tumor microenvironment of human UCB. This result is supported by previous reports of the association of IL-6 and TAM/CAF induction [34–36].

Two-dimensional (2D) monolayer cell culture is a simple method; however, it does not reflect physiological conditions. In this study, we tried the 3D co-culture method of cancer cells and TAMs/CAFs to recognize the cell-to-cell adhesion between UCB cells and stromal cells. Cancer cells and TAMs/CAFs form multicellular mixed spheroids in which cells are exposed to a gradient of hypoxia, thus reflecting the actual human tumor biology more closely than that by 2D co-culture. UCB is one of the most hypoxic solid tumors, and HIF-1α levels are higher in cancer tissue than in normal urothelial tissue [37]. Here, we found that that CXCL1 produced in TAMs and CAFs acted in a paracrine fashion and exhibited enhanced cell-to-cell adhesion of TAMs/CAFs with cancer cells.

Desmoplasia comprises a dense stromal fibro-inflammatory reaction of fibroblasts, inflammatory cells, and tumor vasculature. Recent studies have suggested that hypoxia and subsequently elevated HIF-1α increase desmoplasia by upregulating the formation of sonic hedgehog ligand by pancreatic cancer cells, which activate hedgehog signaling and stimulate the formation of collagen I and fibronectin by fibroblast cells [38]. This phenomenon can facilitate close pro-tumorigenic communication between cancer cells and stromal cells, resulting in limiting drug delivery and chemoresistance due to promotion of desmoplasia.

We used 2 different *in vivo* approaches for confirming the role of CXCL1 produced in TAMs and CAFs around the cancer cells: the subcutaneous xenograft model and the orthotopic bladder tumor model. As we hypothesized, CXCL1 produced in TAMs and CAFs played critical roles in tumor growth and cell implantation, respectively (Figure 5A–G). Interestingly, higher numbers of tumor-infiltrating TAMs and CAFs around the tumors were linked with a higher risk of intravesical recurrence (Figure 5H). In the management of NMIBC, appropriate control for intravesical recurrence after TURBT is as important as control of disease progression. Multifocality and frequent recurrence are characteristic features of UCB and UC of the upper urinary tract. Many of the intravesical recurrences are not life-threatening but can affect the patient's quality of life because intravesical recurrence requires repeated treatments, including TURBT. Previous molecular studies based on IHC, loss of heterozygosity, and mutation analysis of *TP53* demonstrated that intraluminal cell seeding might be an important mechanism of multifocal occurrence and UCB recurrence [39,40]. Our findings suggested that inhibition of CXCL1 signaling between

cancer cells and stromal cells may reduce the risk of intravesical recurrence after TURBT.

On the basis of our results, we propose the mechanism whereby CXCL1 exerts a crucial influence on human UCB (Figure 6). CXCL1 is expressed in human UCB, especially in high-grade and high-stage tumors, and is secreted to the stromal area or bloodstream. The chemotactic roles of CXCL1 and IL-6, as well as hypoxic conditions, induce and recruit TAMs and CAFs into the tumoral area, leading to the assemblage of tumor microenvironment-favoring cancer cells [41,42]. Both TAMs and CAFs supply CXCL1 and other growth factors to cancer cells in return, which promotes close communication and interaction between cancer cells and TAMs/CAFs. As a result, CXCL1 signaling in the tumor microenvironment may be responsible for repeated intravesical recurrence and disease progression. Disrupting this signaling pathway provides an alternative approach for the treatment of the CXCL1-dependent drive in UCB and may also help to enhance the delivery of chemotherapy.

Conclusion

Knowledge of the actual involvement of these stromal cells in the development of UCB will facilitate the search for new therapies targeting the stromal component of bladder cancers. Inhibiting CXCL1 signaling, which can lead to the aberrant regulation of this chemokine, is a promising therapeutic approach for human UCB. Currently, there is no available inhibitor of CXCL1 in the clinical setting. Novel small-molecule inhibitors, neutralizing antibodies, or anti-sense nucleotides disrupting CXCL1 signaling need to be developed and tested in patients with bladder cancer refractive to conventional therapies.

Supplementary data to this article can be found online at http://dx.doi.org/10.1016/j.neo.2016.08.002.

Conflicts of Interest

We declare that we have no conflicts of interest.

Acknowledgement

This work was supported by JSPS KAKENHI Grant Number 26861290 (M.M.), 15K10605 (K.F.) and Fiscal Years 2015–2016 Nara Medical University Grant-in-Aid for Collaborative Research Projects (K.F. and M.M.).

Reference

[1] Siegel R, Ma J, Zou Z, and Jemal A (2014). Cancer statistics, 2014. *CA Cancer J Clin* **64**, 9–29.

[2] Miyake M, Gotoh D, Shimada K, Tatsumi Y, Nakai Y, Anai S, Torimoto K, Aoki K, Tanaka N, Konishi N, et al (2015). Exploration of risk factors predicting outcomes for primary T1 high-grade bladder cancer and validation of the Spanish Urological Club for Oncological Treatment scoring model: Long-term follow-up experience at a single institute. *Int J Urol* **22**, 541–547.

[3] Hanahan D and Weinberg RA (2011). Hallmarks of cancer: the next generation. *Cell* **144**, 646–674.

[4] Stadler M, Walter S, Walzl A, Kramer N, Unger C, Scherzer M, Unterleuthner D, Hengstschläger M, Krupitza G, and Dolznig H (2015). Increased complexity in carcinomas: Analyzing and modeling the interaction of human cancer cells with their microenvironment. *Semin Cancer Biol* **35**, 107–124.

[5] Miyake M, Lawton A, Goodison S, Urquidi V, Gomes-Giacoia E, Zhang G, Ross S, Kim J, and Rosser CJ (2013). Chemokine (C-X-C) ligand 1 (CXCL1) protein expression is increased in aggressive bladder cancers. *BMC Cancer* **13**, 322.

[6] Miyake M, Lawton A, Goodison S, Urquidi V, and Rosser CJ (2014). Chemokine (C-X-C motif) ligand 1 (CXCL1) protein expression is increased in high-grade prostate cancer. *Pathol Res Pract* **210**, 74–78.

[7] Miyake M, Goodison S, Urquidi V, Gomes Giacoia E, and Rosser CJ (2013). Expression of CXCL1 in human endothelial cells induces angiogenesis through the CXCR2 receptor and the ERK1/2 and EGF pathways. *Lab Investig* **93**, 768–778.

[8] Mantovani A and Sica A (2010). Macrophages, innate immunity and cancer: balance, tolerance, and diversity. *Curr Opin Immunol* **22**, 231–237.

[9] Komohara Y, Jinushi M, and Takeya M (2014). Clinical significance of macrophage heterogeneity in human malignant tumors. *Cancer Sci* **105**, 1–8.

[10] Hao NB, Lü MH, Fan YH, Cao YL, Zhang ZR, and Yang SM (2012). Macrophages in tumor microenvironments and the progression of tumors. *Clin Dev Immunol*, 948098.

[11] Komohara Y, Hasita H, Ohnishi K, Fujiwara Y, Suzu S, Eto M, and Takeya M (2011). Macrophage infiltration and its prognostic relevance in clear cell renal cell carcinoma. *Cancer Sci* **102**, 1424–1431.

[12] Sugimoto M, Mitsunaga S, Yoshikawa K, Kato Y, Gotohda N, Takahashi S, Konishi M, Ikeda M, Kojima M, Ochiai A, et al (2014). Prognostic impact of M2 macrophages at neural invasion in patients with invasive ductal carcinoma of the pancreas. *Eur J Cancer* **50**, 1900–1908.

[13] Wang B, Liu H, Dong X, Wu S, Zeng H, Liu Z, Wan D, Dong W, He W, Chen X, et al (2015). High CD204+ tumor-infiltrating macrophage density predicts a poor prognosis in patients with urothelial cell carcinoma of the bladder. *Oncotarget* **6**, 20204–20214.

[14] Shigeoka M, Urakawa N, Nakamura T, Nishio M, Watajima T, Kuroda D, Komori T, Kakeji Y, Semba S, and Yokozaki H (2013). Tumor associated macrophage expressing CD204 is associated with tumor aggressiveness of esophageal squamous cell carcinoma. *Cancer Sci* **104**, 1112–1119.

[15] Xouri G and Christian S (2010). Origin and function of tumor stroma fibroblasts. *Semin Cell Dev Biol* **21**, 40–46.

[16] Xing F, Saidou J, and Watabe K (2010). Cancer associated fibroblasts (CAFs) in tumor microenvironment. *Front Biosci* **15**, 166–179.

[17] Mishra P, Banerjee D, and Ben-Baruch A (2011). Chemokines at the crossroads of tumor-fibroblast interactions that promote malignancy. *J Leukoc Biol* **89**, 31–39.

[18] Kharaishvili G, Simkova D, Bouchalova K, Gachechiladze M, Narsia N, and Bouchal J (2014). The role of cancer-associated fibroblasts, solid stress and other microenvironmental factors in tumor progression and therapy resistance. *Cancer Cell Int* **14**, 41.

[19] Paulsson J and Micke P (2014). Prognostic relevance of cancer-associated fibroblasts in human cancer. *Semin Cancer Biol* **25**, 61–68.

[20] Herrera M, Herrera A, Domínguez G, Silva J, García V, García JM, Gómez I, Soldevilla B, Muñoz C, Provencio M, et al (2013). Cancer-associated fibroblast and M2 macrophage markers together predict outcome in colorectal cancer patients. *Cancer Sci* **104**, 437–444.

[21] Tsujino T, Seshimo I, Yamamoto H, Ngan CY, Ezumi K, Takemasa I, Ikeda M, Sekimoto M, Matsuura N, and Monden M (2007). Stromal myofibroblasts predict disease recurrence for colorectal cancer. *Clin Cancer Res* **13**, 2082–2090.

[22] Nakayama H, Enzan H, Miyazaki E, Naruse K, Kiyoku H, and Hiroi M (1998). The role of myofibroblasts at the tumor border of invasive colorectal adenocarcinomas. *Jpn J Clin Oncol* **28**, 615–620.

[23] Miyake M, Goodison S, Lawton A, Gomes-Giacoia E, and Rosser CJ (2015). Angiogenin promotes tumoral growth and angiogenesis by regulating matrix metallopeptidase-2 expression via the ERK1/2 pathway. *Oncogene* **34**, 890–901.

[24] Nogawa M, Yuasa T, Kimura S, Tanaka M, Kuroda J, Sato K, Yokota A, Segawa H, Toda Y, Kageyama S, et al (2005). Intravesical administration of small interfering RNA targeting PLK-1 successfully prevents the growth of bladder cancer. *J Clin Invest* **115**, 978–985.

[25] Heneberg P (2016). Paracrine tumor signaling induces transdifferentiation of surrounding fibroblasts. *Crit Rev Oncol Hematol* **97**, 303–311.

[26] Carosella ED, Ploussard G, LeMaoult J, and Desgrandchamps F (2015). A Systematic Review of Immunotherapy in Urologic Cancer: Evolving Roles for Targeting of CTLA-4, PD-1/PD-L1, and HLA-G. *Eur Urol* **68**, 267–279.

[27] Carthon BC, Wolchok JD, Yuan J, Kamat A, Ng Tang DS, Sun J, Ku G, Troncoso P, Logothetis CJ, Allison JP, et al (2010). Preoperative CTLA-4 blockade: tolerability and immune monitoring in the setting of a presurgical clinical trial. *Clin Cancer Res* **16**, 2861–2871.

[28] Powles T, Eder JP, Fine GD, Braiteh FS, Loriot Y, Cruz C, Bellmunt J, Burris HA, Petrylak DP, Teng SL, et al (2014). MPDL3280A (anti-PD-L1) treatment leads to clinical activity in metastatic bladder cancer. *Nature* **515**, 558–562.

[29] Acharyya S, Oskarsson T, Vanharanta S, Malladi S, Kim J, Morris PG, Manova-Todorova K, Leversha M, Hogg N, Seshan VE, et al (2012). A CXCL1 paracrine network links cancer chemoresistance and metastasis. *Cell* **150**, 165–178.

[30] Kalluri R and Zeisberg M (2006). Fibroblasts in Cancer. *Nat Rev Cancer* **6**, 392–401.

[31] Sato H, Takino T, Okada Y, Cao J, Shinagawa A, Yamamoto E, and Seiki M (1994). A matrix metalloproteinase expressed on the surface of invasive tumour cells. *Nature* **370**, 61–65.

[32] Erler JT, Bennewith KL, Cox TR, Lang G, Bird D, Koong A, Le QT, and Giaccia AJ (2009). Hypoxia-induced lysyl oxidase is a critical mediator of bone marrow cell recruitment to form the premetastatic niche. *Cancer Cell* **15**, 35–44.

[33] Osuala KO, Sameni M, Shah S, Aggarwal N, Simonait ML, Franco OE, Hong Y, Hayward SW, Behbod F, Mattingly RR, et al (2015). Il-6 signaling between ductal carcinoma in situ cells and carcinoma-associated fibroblasts mediates tumor cell growth and migration. *BMC Cancer* **15**, 584.

[34] Maniecki MB, Etzerodt A, Ulhøi BP, Steiniche T, Borre M, Dyrskjøt L, Orntoft TF, Moestrup SK, and Møller HJ (2012). Tumor-promoting macrophages induce the expression of the macrophage-specific receptor CD163 in malignant cells. *Int J Cancer* **131**, 2320–2331.

[35] Konur A, Kreutz M, Knüchel R, Krause SW, and Andreesen R (1998). Cytokine repertoire during maturation of monocytes to macrophages within spheroids of malignant and non-malignant urothelial cell lines. *Int J Cancer* **78**, 648–653.

[36] Yeh CR, Hsu I, Song W, Chang H, Miyamoto H, Xiao GQ, Li L, and Yeh S (2015). Fibroblast ERα promotes bladder cancer invasion via increasing the CCL1 and IL-6 signals in the tumor microenvironment. *Am J Cancer Res* **5**, 1146–1157.

[37] Ioachim E, Michael M, Salmas M, Michael MM, Stavropoulos NE, and Malamou-Mitsi V (2006). Hypoxia-inducible factors HIF-1alpha and HIF-2alpha expression in bladder cancer and their associations with other angiogenesis-related proteins. *Urol Int* **77**, 255–263.

[38] Spivak-Kroizman TR, Hostetter G, Posner R, Aziz M, Hu C, Demeure MJ, Von Hoff D, Hingorani SR, Palculict TB, Izzo J, et al (2013). Hypoxia triggers hedgehog-mediated tumor-stromal interactions in pancreatic cancer. *Cancer Res* **73**, 3235–3247.

[39] Hafner C, Knuechel R, Zanardo L, Dietmaier W, Blaszyk H, Cheville J, Hofstaedter F, and Hartmann A (2001). Evidence for oligoclonality and tumor spread by intraluminal seeding in multifocal urothelial carcinomas of the upper and lower urinary tract. *Oncogene* **20**, 4910–4915.

[40] Hafner C, Knuechel R, Stoehr R, and Hartmann A (2002). Clonality of multifocal urothelial carcinomas: 10 years of molecular genetic studies. *Int J Cancer* **101**, 1–6.

[41] Schioppa T, Uranchimeg B, Saccani A, Biswas SK, Doni A, Rapisarda A, Bernasconi S, Saccani S, Nebuloni M, Vago L, et al (2003). Regulation of the chemokine receptor CXCR4 by hypoxia. *J Exp Med* **198**, 1391–1402.

[42] Levental KR, Yu H, Kass L, Lakins JN, Egeblad M, Erler JT, Fong SF, Csiszar K, Giaccia A, Weninger W, et al (2009). Matrix crosslinking forces tumor progression by enhancing integrin signaling. *Cell* **139**, 891–906.